Hindawi
Complexity
Volume 2019, Article ID 3827201, 18 pages
https://doi.org/10.1155/2019/3827201

Research Article

Adaptive Multi-Switching Synchronization of High-Order Memristor-Based Hyperchaotic System with Unknown Parameters and Its Application in Secure Communication

Zhili Xiong,[1,2] **Shaocheng Qu**,[1] **and Jing Luo**[1]

[1]*Department of Electronics and Information Engineering, Central China Normal University, Wuhan 430079, China*
[2]*School of Physics and Electric Information, Huanggang Normal University, Huanggang 438000, China*

Correspondence should be addressed to Shaocheng Qu; qushaocheng@mail.ccnu.edu.cn

Received 19 May 2019; Revised 24 June 2019; Accepted 4 July 2019; Published 19 December 2019

Guest Editor: Lazaros Moysis

This article investigates an adaptive multi-switching synchronization for two identical high-order memristor-based hyperchaotic systems with uncertain parameters. Firstly, the dynamic characteristics of two high-order memristor hyperchaotic systems with uncertain parameters are analyzed. Then, an adaptive multi-switching controller is designed to realize the multi-switching synchronization of the two high-order hyperchaotic systems, and the unknown parameters of the systems are identified to their true values. Furthermore, numerical simulation results testify the effectiveness of the proposed strategy. Finally, the proposed algorithm applied in secure communication of masking encryption and image encryption is validated by statistical analysis.

1. Introduction

Chaos is a kind of irregular and unstable motion state existing in nonlinear system. And it has three properties: infinite recurrence, bondedness, and sensitivity to initial conditions. Since the slight change of the initial state value will result in a large error in the chaotic system, chaos was considered to be harmful until Pecora and Carrol proposed the concept of chaos synchronization in 1990, the synchronization of two coupled chaotic oscillators is observed for the first time [1]. Chaos synchronization means that the motion trajectory of one system converges to the trajectory of another system and is always consistent. The synchronization of chaotic systems has drawn attentions in many fields including secure communication [2–4], electrical engineering, and biological system [5]. In practical engineering, there exists partially or fully uncertain parameters in drive or response systems, the conventional control methods can not be applied to synchronize the two chaotic systems with uncertainties. Hence, a number of control methods have been studied to accomplish two chaos synchronization with unknown parameters or uncertain terms, such as sliding mode control method [6–8], impulsive control [9], fuzzy control scheme [10, 11], and adaptive strategies [6, 12–14]. The adaptive synchronization for uncertain chaotic system was proposed by Parlitz firstly, the identification method of the adaptive synchronization was employed to estimation the unknown parameters in Lorenz system [15]. Later, this strategy has been extended to other uncertain chaotic systems. Adaptive synchronization methods for a class of chaotic systems existing in the literature are studied in [16]. However, the linear independence condition for some chaotic systems with unknown parameters is neglected to guarantee the true convergence of the estimated parameters. Reference [17] described the principle of the linear independence, the functions $f_i(t)\,(i = 1, 2, \cdots, n)$ are said to be linear independent if there do not exist nonzero constants $\alpha_i\,(i = 1, 2, \cdots, n)$, such that $f_1(t)\alpha_1 + f_2(t)\alpha_2 + \cdots + f_n(t)\alpha_n = 0$.The adaptive multi-switching synchronization was proven to be effective to solve the identification of the unknown parameters in [18].

Multi-switching synchronization proposed by Ucar can provide more combined error spaces [19], it is beneficial to prevent intruders from gaining useful informations of the chaotic synchronization system. Although multi-switching synchronization is suitable to enhance anti-attack and resistance for secure communication, only a few literatures for it have been proposed [20–24]. Wang and S investigated the

multi-switching synchronization of chaotic systems with unknown parameters by the adaptive control techniques [20]. Ahmad et al. implemented multi-switching combination synchronization for three chaotic systems, and introduced its application in secure communication [21]. Wen et al. addressed adaptive control method to accomplish multi-switching combination synchronization of three nonidentical chaotic systems with unknown parameters [22]. Khan et al. designed a multi-switching synchronization strategy for different switches of three masters and one slave hyperchaotic system [23]. Prajapati et al. completed multi-switching compound synchronization of four different chaotic systems [24]. Above these analysis, these chaotic or hyperchaotic systems are 3D or 4D systems without considering memristors. It will be a challenging task to study chaotic synchronization with memristor. Hence, the adaptive multi-switching synchronization can be extend to the memristor-based systems with unknown parameters.

The memristor is one of three breakthrough inventions of Chua in the nonlinear control systems. In 1971, Chua conceived the notion of memristors based on the principle of symmetry and signal integrity analysis, and considered memristors to be the fourth circuit component following capacitors, resistors, and inductors [25]. The researches on memristor have attract significant attentions only recently after the realization of TiO_2-based physical memristor by the HP Laboratories in 2008 [26]. Itoh and Chua developed memristor oscillators which was a kind of typical memristor-based chaotic system [27]. In recent years, many researches on memristor have attracted the attention of scholars [10, 11, 13, 14, 28–32]. Wen et al. designed an adaptive controller to solve the synchronization problem of the memristor-based Chua circuit. Wen et al. established a fuzzy modeling and proposed a fuzzy controller to solve the synchronization of different memristor-based chaotic systems [10]. Wang et al. designed and analyzed the adaptive synchronization for two flux-controlled 5D memristor chaotic systems, but the unknown parameters of the systems can not be identified to the true value for the linear independence condition. In [31], the analysis of the linear dependence condition for the parameter identification is followed as

$$\begin{aligned}
\dot{e}_1 &= (a - \hat{a}(t))(e_2 - e_1) - k_1 e_1,\\
\dot{e}_2 &= -k_2 e_2,\\
\dot{e}_3 &= \left(\hat{b}(t) - b\right) e_3 - k_3 e_3,\\
\dot{e}_4 &= -k_4 e_4,\\
\dot{e}_5 &= -k_5 e_5.
\end{aligned} \tag{1}$$

Finally, it is clear that $e_1 = 0|_{t\to\infty}$, $e_2 = 0|_{t\to\infty}$, $e_3 = 0|_{t\to\infty}$, $e_4 = 0|_{t\to\infty}$, $e_5 = 0|_{t\to\infty}$with the realization of synchronization between the drive system and the response system. We know $a - \hat{a}(t) = const1$ and $\hat{b}(t) - b = const2$ according to linear independence, where the constant numbers $consti\,(i = 1, 2)$ can be arbitrary values. Hence, the unknown parameters can not be identified to the true values. Based on the above analysis, memristor-based chaotic system synchronization has been widely studied [2, 8, 13, 33], but there are few literatures on the synchronization of memristor chaotic systems with considering the linear independence of unknown parameters, the unknown parameters can not be identified the true values. In order to solve the problem of unknown parameter identification, the adaptive multi-switching synchronization is extent to employ in the high-order memristor-based hyperchaotic systems with unknown parameters.

Due to the sensitivity of initial states, unpredictability and the pseudo-random property, memristor-based chaotic systems are suitable for secure communication. The useful signals can be hidden in chaotic signals to prevent being hacked and modified. However, the image encryption process involves a large amount of image data, it is difficult to accomplish image encryption by the traditional encryption techniques, such as RSA algorithm, IDEA, and AES. Therefore, researchers and engineers are committed to the researches of the new image encryption algorithm to enhance the information security. Sun et al. proposed an adaptive controller to realize compound synchronization among 4D chaotic oscillator systems and presented a secure communication method based on Chaotic Synchronization [2]. Li et al. analyzed the dynamic characteristics of memristor-based chaotic system and applied chaotic sequences of the new system to secure communication [34]. However, the literature of multi-switch synchronization for high-order memristor-based hyperchaotic systems with unknown parameters appears less, especially its application in secure communication.

Motivated from the above analysis, the adaptive multi-switching controller is designed to realize the synchronization for high-order memristor hyperchaotic systems with uncertain parameters and its corresponding applications in secure communication. The main contributions of this paper are as follows:

(1) The principle of linear independence is introduced. By the analysis of the linear independence condition for the system in [31], the unknown parameters can be arbitrary values and failed to be identified to their true values.

(2) The nonlinear dynamic characteristics of the high-order memristor-based hyperchaotic systems which has two Lyapunov exponents are analyzed.

(3) In order to solve the problem of the parameter identification in [31], the adaptive multi-switching synchronization scheme is proposed in the paper, the numerical results show that the master-slave system can be synchronized and the unknown parameters can be consistent with the given value simultaneously.

(4) The adaptive multi-switching synchronization can offer various different dynamic errors of the master-slave hyperchaotic system, which is suitable for secure communication. An encryption algorithm based on multi-switching synchronization hyperchaotic system with memristor is presented, by the gray histogram and correlation analysis, the numerical simulation results reflect that the proposed method improved the security to prevent intruders from cracking and tampering during the process of information transmission.

The organization of this paper lists as follows. Section 2 analyzes the adaptive multi-switching synchronization strategy. Section 3 implements the adaptive multi-switching synchronization for high-order memristor hyperchaotic systems with unknown parameters, and validates the feasibility and effectiveness of the proposed strategy by using numerical simulations. Section 4 proposes a new encryption algorithm based on proposed strategy to improve the security of the useful signals, and introduces the statistical analysis methods of the gray histogram and correlation. Finally, Section 5 draws the conclusion and prospects further works.

2. Problem Formulation

In this section, an adaptive multi-switching synchronization strategy is introduced for master-slave chaotic system with unknown parameters.

Considering three n-dimensional hyperchaotic systems with unknown parameters, the two master hyperchaotic systems are given by

$$\begin{cases} \dot{v}_1(t) = f_{11}(v_1, v_2, \ldots, v_n) + F_{11}(v_1, v_2, \ldots, v_n)\psi_1, \\ \dot{v}_2(t) = f_{12}(v_1, v_2, \ldots, v_n) + F_{12}(v_1, v_2, \ldots, v_n)\psi_2, \\ \vdots \\ \dot{v}_n(t) = f_{1n}(v_1, v_2, \ldots, v_n) + F_{1n}(v_1, v_2, \ldots, v_n)\psi_n, \end{cases} \tag{2}$$

and

$$\begin{cases} \dot{w}_1(t) = f_{21}(w_1, w_2, \ldots, w_n) + F_{21}(w_1, w_2, \ldots, w_n)\gamma_1, \\ \dot{w}_2(t) = f_{22}(w_1, w_2, \ldots, w_n) + F_{22}(w_1, w_2, \ldots, w_n)\gamma_2, \\ \vdots \\ \dot{w}_n(t) = f_{2n}(w_1, w_2, \ldots, w_n) + F_{2n}(w_1, w_2, \ldots, w_n)\gamma_n, \end{cases} \tag{3}$$

where $v(t) = [v_1, v_2, ..., v_n]^T$, and $w(t) = [w_1, w_2, ..., w_n]^T$ are the state vectors. $f_{1i}(v) = (f_{11}(v), f_{12}(v), \cdots, f_{1n}(v))^T$ and $f_{2i}(v) = (f_{21}(v), f_{22}(v), \cdots, f_{2n}(v))^T$ are nonlinear vector terms from $R^n \to R^n$, $F(v_{1i}) \in R^{n\times n}$ and $F(v_{2i}) \in R^{n\times n}$ are the system matrices, and $\psi, \gamma \in R^n$ are unknown vector parameters.

The slave hyperchaotic system is described by

$$\begin{cases} \dot{z}_1(t) = g_1(z_1, z_2, \ldots, z_n) + G_1(z_1, z_2, \ldots, z_n)\eta_1 + u_1, \\ \dot{z}_2(t) = g_2(z_1, z_2, \ldots, z_n) + G_2(z_1, z_2, \ldots, z_n)\eta_2 + u_2, \\ \vdots \\ \dot{z}_n(t) = g_n(z_1, z_2, \ldots, z_n) + G_n(z_1, z_2, \ldots, z_n)\eta_n + u_n, \end{cases} \tag{4}$$

where $z(t) = [z_1, z_2, \ldots, z_n]^T$ is a state vector, $g(z) = (g_1(z), g_1(z), \ldots, g_1(z))^T$ is a nonlinear vector function from $R^n \to R^n$, $G(z) \in R^{n\times n}$ is a system matrix, and $\eta \in R^n$ is an unknown vector parameter, and $U = (u_1, u_2, \cdots, u_n)$ is a controller to be designed for the synchronization of master-slave hyperchotic systems.

Definition 1. The slave system (3) will realize the synchronization with the two master systems (1) and (2), if there exist diagonal matrices C, D, $H \in R^{n\times n}$, and $H \neq 0$, such that

$$\lim_{t\to\infty} \|e\| = \lim_{t\to\infty} \|Cv + Dw - Hz\| = 0, \tag{5}$$

where $\|\cdot\|$ represents the Euclidean norm, and $e = Cv + Dw - Hz$ is the error vector of the synchronization with master-slave systems.

Remark 1. Assume the scaling matrices C, D, H as $C = diag(c_1, c_2, \cdots, c_n)$, $D = diag(d_1, d_2, \cdots, d_n)$, and $H = diag(h_1, h_2, \cdots, h_n)$ respectively. The error vectors are obtained as $e_{ijk} = c_i v_i + d_j w_j - h_k z_k$. In accordance with the Definition 1, $i = j = k$, $i \neq j = k$, $i = j \neq k$, $(i, j, k = 1, 2, \ldots, n)$. According to (1)–(4), the error dynamics is gain by

$$\begin{aligned} \dot{e} = {} & Cf_1(v) + CF_1(v)\psi + Df_2(w) + DF_2(w)\gamma \\ & - Hg(z) - HG(z)\eta - HU. \end{aligned} \tag{6}$$

Now, in order to achieve the synchronization of the master-slave systems, an appropriate controller U and the unknown parameters ψ, γ, and η need to design.

$\hat{\psi}$, $\hat{\gamma}$, and $\hat{\eta}$ are the estimated values of the parameters ψ, γ and η respectively.

Define the estimated error parameters as

$$\tilde{\psi} = \psi - \hat{\psi}, \tilde{\gamma} = \gamma - \hat{\gamma}, \tilde{\eta} = \eta - \hat{\eta}. \tag{7}$$

Then,

$$\dot{\tilde{\psi}} = -\dot{\hat{\psi}}, \dot{\tilde{\gamma}} = -\dot{\hat{\gamma}}, \dot{\tilde{\eta}} = -\dot{\hat{\eta}}. \tag{8}$$

Theorem 1. *The controller U is selected as*

$$\begin{aligned} U = {} & H^{-1}Cf_1(v) + H^{-1}CF_1(v)\hat{\psi} + H^{-1}Df_2(w) + H^{-1}DF_2(w)\hat{\gamma} - g(z) \\ & - G(z)\hat{\eta} + H^{-1}e + H^{-1}\mathrm{sgn}(e)|e|^{\mu}, \end{aligned} \tag{9}$$

where $\mathrm{sgn}(e)$ *expresses signum function. The parameter update laws are designed as*

$$\dot{\hat{\psi}} = F_1(v)^T Ce, \dot{\hat{\gamma}} = F_2(w)^T De, \dot{\hat{\eta}} = G(z)^T He. \tag{10}$$

Proof. The Lyapunov function is selected as

$$V(t) = \frac{1}{2}\left(e^T e + \tilde{\psi}^T\tilde{\psi} + \tilde{\gamma}^T\tilde{\gamma} + \tilde{\eta}^T\tilde{\eta}\right), \tag{11}$$

Then,

$$\dot{V}(t) = \dot{e}^T e - \tilde{\psi}^T\dot{\hat{\psi}} - \tilde{\gamma}^T\dot{\hat{\gamma}} - \tilde{\eta}^T\dot{\hat{\eta}}. \tag{12}$$

Substituting (6–10) into (12) gains as

$$\begin{aligned} \dot{V}(t) &= \left[Cf_1(v) + CF_1(v)\psi + Df_2(w) + DF_2(w)\gamma - Hg(z) - HG(z)\eta - HU\right]^T e - \tilde{\psi}^T\dot{\hat{\psi}} - \tilde{\gamma}^T\dot{\hat{\gamma}} - \tilde{\eta}^T\dot{\hat{\eta}}, \\ &= \left[CF_1(v)(\psi - \hat{\psi}) + DF_2(w)(\gamma - \hat{\gamma}) - HG(z)(\eta - \hat{\eta}) - e - \mathrm{sgn}(e)|e|^{\mu}\right]^T e - \tilde{\psi}^T\dot{\hat{\psi}} - \tilde{\gamma}^T\dot{\hat{\gamma}} - \tilde{\eta}^T\dot{\hat{\eta}}, \\ &= \left[CF_1(v)\tilde{\psi} + DF_2(w)\tilde{\gamma} - HG(z)\tilde{\eta} - e - \mathrm{sgn}(e)|e|^{\mu}\right]^T e - \tilde{\psi}^T\dot{\hat{\psi}} - \tilde{\gamma}^T\dot{\hat{\gamma}} - \tilde{\eta}^T\dot{\hat{\eta}}, \\ &= \tilde{\psi}^T\left(F_1(v)^T Ce - \dot{\hat{\psi}}\right) + \tilde{\gamma}^T\left(F_2(w)^T De - \dot{\hat{\gamma}}\right) + \tilde{\eta}^T\left(G(z)^T He - \dot{\hat{\eta}}\right) - e^T e - |e|^{\mu+1}, \\ &= -e^T e - |e|^{\mu+1}. \end{aligned} \tag{13}$$

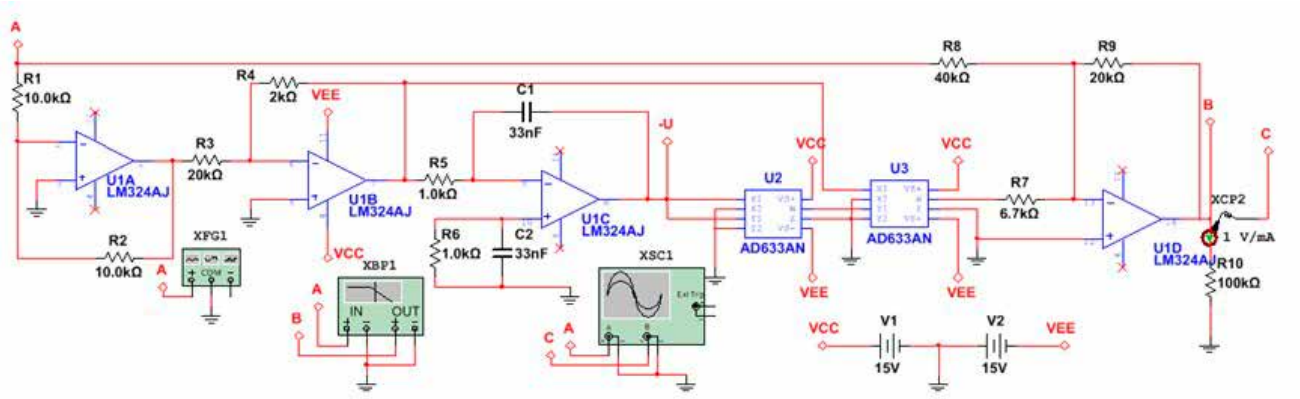

Figure 1: The equivalent circuit of the flux-controlled smooth cubic memristor.

Thus, we can know $\dot{V}(t) < 0$. In the light of the Lyapunov stability theory, if $V(t) > 0$ and $\dot{V}(t) < 0$, the master system will synchronize with the slave system.

Remark 2. If $C = 0$ or $D = 0$, the synchronization problem becomes multi-switching modified projective synchronization. If $C = 0$ or $D = 0$ and $H = 1$, the synchronization problem turns into multi-switching synchronization. In order to facilitate the analysis of multi-switch synchronization of complex systems, the parameters $C = 1$, $D = 0$, and $H = 1$ are selected in the following sections.

3. Adaptive Multi-Switching Synchronization of High-Order Memristor-Based Hyperchaotic System

In this section, firstly, the 5D hyperchaotic system with memristor is introduced. Secondly, two identical 5D memristor hyperchaotic systems with unknown parameters are composited a master-slave system. Thirdly, an adaptive multi-switching synchronization strategy is proposed for the system. Finally, the numerical simulation results indicate that the synchronization of the master-slave system can be implemented, and unknown parameters of the system can be identified to their given values.

3.1. High-Order Memristor-Based Hyperchaotic System. Memristors represent the relationship between magnetic flux φ and charge q which is a missing circuit component with memory characteristic conceived by Chua in 1971 [25]. The function between the magnetic flux and the charge passing the memristor is not unique. Select a smooth cubic memristor [35] which can be expressed as

$$q(\varphi) = \alpha\varphi + \beta\varphi^3, \tag{14}$$

and

$$W(\varphi) = \frac{dq(\varphi)}{d\varphi} = \alpha + 3\beta\varphi^2, \tag{15}$$

where α and β are positive parameters.

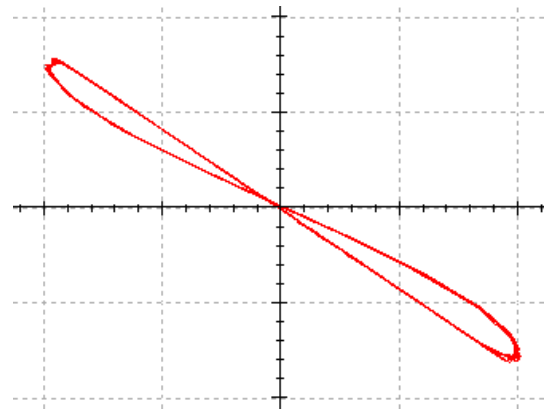

Figure 2: Flux-controlled memristors characteristics.

In line with the above defined flux-controlled memristor formula (14), an equivalent circuit with a smooth cubic memristor is shown in Figure 1, where a = 0.1, b = 0.01 (input is 1 V 100 Hz sinusoidal wave). Circuit diagram of C1 = C2 = 33 nf, R1 = R2 = 10 kΩ, R3 = R9 = 20 kΩ, R4 = 2 kΩ, R5 = R6 = 1 kΩ, R7 = 6.7 kΩ, R8 = 40 kΩ, R10 = 100 kΩ. The circuit consists of operational amplifiers, multipliers, resistors, and capacitors. The first and second stage operational amplifiers are used for signal reduction. The third pole operational amplifier using differential integrator prevents "zero drift". Tow multipliers perform simulated multiplication. The fourth operational amplifier performs reverse addition.

Memristor is a nonlinear resistor with charge memory function. Applying an arbitrary periodic voltage signal to the ideal memristor, the V-I characteristics of the excitation voltage and the corresponding response current can be depicted as a skewed "8" shaped pinched hysteresis loop in Figure 2.

The model originated from wang's 5D hyperchaotic system [31] is as follows:

$$\begin{aligned}
\dot{x}_1 &= a(x_2 - x_1) + 4x_2x_3 - kx_1W(x_5),\\
\dot{x}_2 &= -x_1 + x_4 + 16x_2 - x_1x_3,\\
\dot{x}_3 &= -bx_3 - x_2x_4 + x_1x_2 - x_1x_5,\\
\dot{x}_4 &= -gx_3x_5 - 10x_2 + 0.15x_1x_3,\\
\dot{x}_5 &= -x_1.
\end{aligned} \tag{16}$$

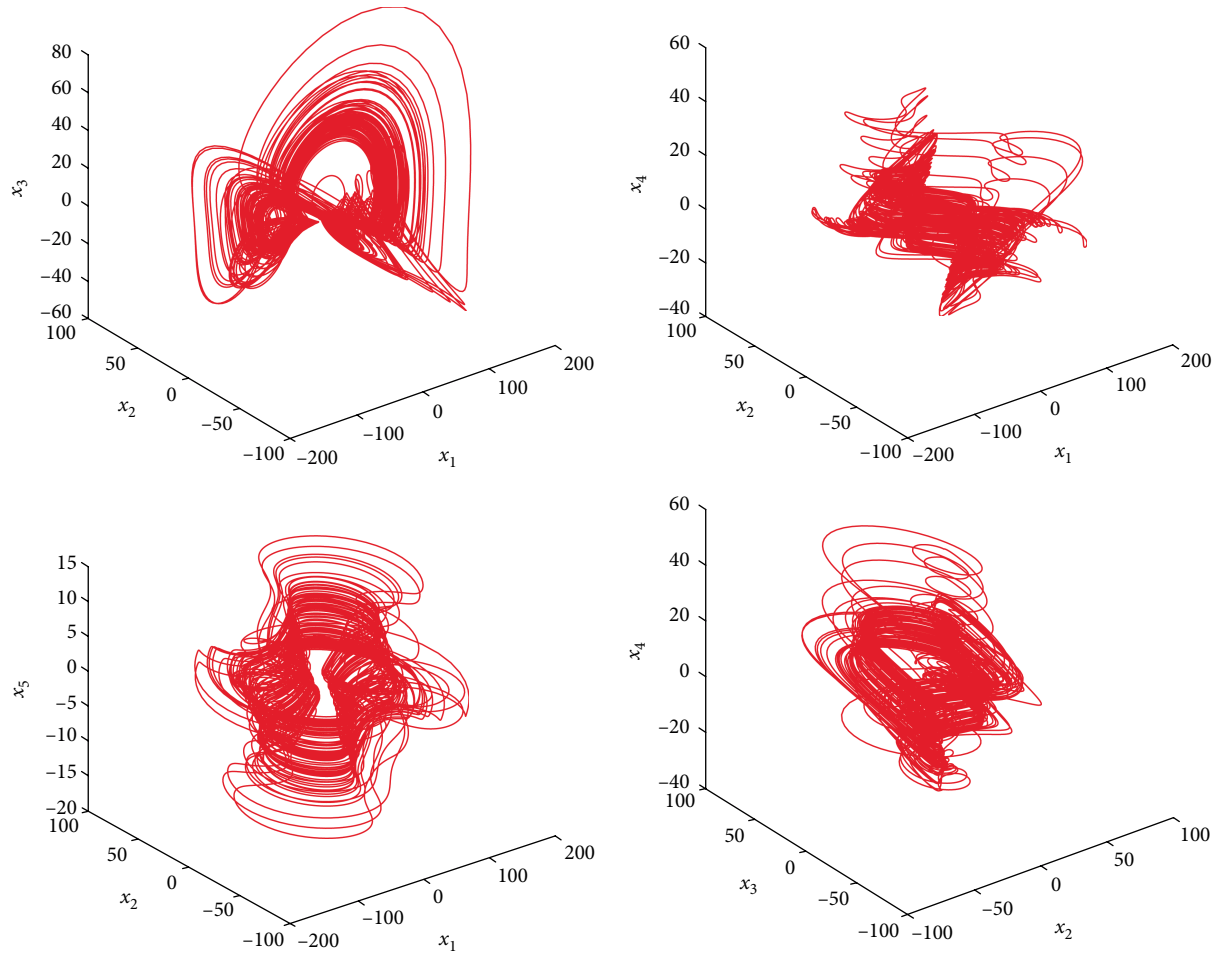

FIGURE 3: 3D phase portraits of the hyperchaotic system.

where $W(x_5)$ is the memristor model, as follows

$$W(x_5) = \alpha + 3\beta {x_5}^2. \tag{17}$$

Substituting (17) into (16) obtains

$$\begin{aligned}
\dot{x}_1 &= a(x_2 - x_1) + 4x_2x_3 - kx_1\left(\alpha + 3\beta {x_5}^2\right),\\
\dot{x}_2 &= -x_1 + 16x_2 - x_1x_3 + x_4,\\
\dot{x}_3 &= -bx_3 + x_1x_2 - x_1x_5 - x_2x_4,\\
\dot{x}_4 &= -10x_2 + 0.15x_1x_3 - gx_3x_5,\\
\dot{x}_5 &= -x_1.
\end{aligned} \tag{18}$$

If the parameters are selected as $a = 14$, $b = 78$, $k = 0.02$, $\alpha = 0.1$, $\beta = 0.01$, $g = 0.3$, and the initial states are given as: $x(0) = [4, 1.2, 0.5, -3.6, 6]$, the Lyapunov exponents of system (17) can be calculated as $L_1 = 0.0137$, $L_2 = 1.0241$, $L_3 = -0.1735$, $L_4 = -2.3787$, and $L_5 = -70.3244$. Two positive Lyapunov exponents indicate that the system is a hyperchaotic system. And its 3D phase portraits and hyperchaotic attractors are shown in Figures 3 and 4 respectively.

Remark 3. In [21–23], third-order chaotic system is as the research object without considering memristor. The high-order hyperchaotic systems with memristor has complex dynamic characteristics, which has attracted attention in engineering practice. It has good application potential in many fields, among them, the research of chaotic synchronization has become a hot spot, especially in secure communication.

3.2. Multi-Switching Synchronization for the 5D Memristor Hyperchaotic System with Unknown Parameters. The multi-switching synchronization process can be extended to several identical schemes or different structures of hyperchaotic system which have unknown parameters.

Here, two identical hyperchaotic systems with uncertain parameters composite the master-slave system.

The master system is represented by

$$\begin{aligned}
\dot{x}_1 &= a(x_2 - x_1) + 4x_2x_3 - kx_1\left(0.1 + 0.03{x_5}^2\right),\\
\dot{x}_2 &= -x_1 + x_4 + 16x_2 - x_1x_3,\\
\dot{x}_3 &= -bx_3 + x_1x_2 - x_2x_4 - x_1x_5,\\
\dot{x}_4 &= -10x_2 - gx_3x_5 + 0.15x_1x_3,\\
\dot{x}_5 &= -x_1.
\end{aligned} \tag{19}$$

The slave system is expressed as

$$\begin{aligned}
\dot{y}_1 &= a(y_2 - y_1) + 4y_2y_3 - ky_1\left(0.1 + 0.03{y_5}^2\right) + U_1,\\
\dot{y}_2 &= -y_1 + y_4 + 16y_2 - y_1y_3 + U_2,\\
\dot{y}_3 &= -by_3 + y_1y_2 - y_2y_4 - y_1y_5 + U_3,\\
\dot{y}_4 &= -10y_2 - gy_3y_5 + 0.15y_1y_3 + U_4,\\
\dot{y}_5 &= -y_1 + U_5.
\end{aligned} \tag{20}$$

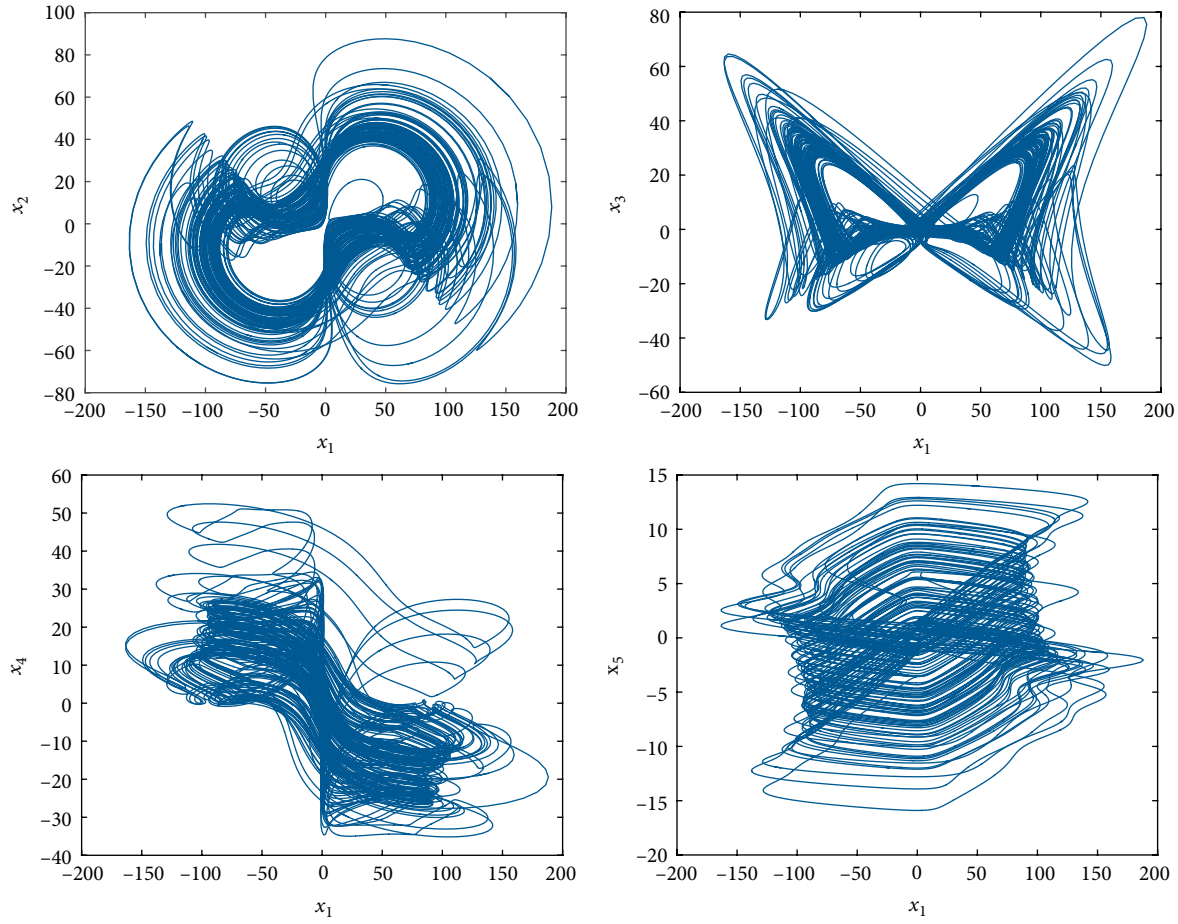

FIGURE 4: 2D projections of the hyperchaotic systems.

According to the Definition 1, the parameters $D = 0$ and $H = 1$ are selected, error system is changed into $e_{ij} = y_j - x_i$, where $i, j = 1, 2, \ldots, 5$.

When $i = j$,

$$e_{11} = y_1 - x_1, e_{22} = y_2 - x_2, \ldots, e_{nn} = y_n - x_n, \quad (21)$$

When $i \neq j$,

$$\begin{aligned} &e_{12} = y_1 - x_2, e_{13} = y_1 - x_3, \ldots, e_{1n} = y_1 - x_n, \\ &e_{21} = y_2 - x_1, e_{23} = y_2 - x_3, \ldots, e_{2n} = y_2 - x_n, \\ &\vdots \\ &e_{n1} = y_n - x_1, e_{n2} = y_n - x_3, \ldots, e_{nn-1} = y_n - x_{n-1}, \end{aligned} \quad (22)$$

From (21) and (22), multiple error systems are obtained, for example:

Switch-1 $e_{13} = y_1 - x_3, e_{22} = y_2 - x_2, e_{31} = y_3 - x_1, e_{44} = y_4 - x_4, e_{55} = y_5 - x_5,$

Switch-2 $e_{12} = y_1 - x_2, e_{34} = y_3 - x_4, e_{23} = y_2 - x_3, e_{51} = y_5 - x_1, e_{45} = y_4 - x_5,$

Switch-3 $e_{12} = y_1 - x_2, e_{13} = y_1 - x_3, e_{14} = y_1 - x_4, e_{15} = y_1 - x_5, e_{21} = y_2 - x_1,$

Switch-4 $e_{11} = y_1 - x_1, e_{22} = y_2 - x_2, e_{33} = y_3 - x_3, e_{44} = y_4 - x_4, e_{55} = y_5 - x_5,$

and so on.

Remark 4. According to the conditions of the two indices $i, j = 1, 2, \ldots, 5$, this section selects two out of the several switches,

Switch-1 $e_{13} = y_1 - x_3, e_{22} = y_2 - x_2, e_{31} = y_3 - x_1, e_{44} = y_4 - x_4, e_{55} = y_5 - x_5,$

Switch-2 $e_{12} = y_1 - x_2, e_{34} = y_3 - x_4, e_{23} = y_2 - x_3, e_{51} = y_5 - x_1, e_{45} = y_4 - x_5.$

Corollary 1. *For switch-1, the dynamic errors are calculated as*

$$\begin{aligned} \dot{e}_{13} &= a(y_2 - y_1) + 4y_2y_3 - ky_1\left(0.1 + 0.03{y_5}^2\right) \\ &\quad + bx_3 - x_1x_2 + x_1x_5 + x_2x_4 + U_1, \\ \dot{e}_{22} &= -y_1 + x_1 + 16e_{22} + e_{24} - y_1y_3 + x_1x_3 + U_2, \\ \dot{e}_{31} &= -by_3 + y_1y_2 - y_1y_5 - y_2y_4 - a(x_2 - x_1) \\ &\quad - 4x_2x_3 - kx_1\left(0.1 + 0.03{x_5}^2\right) + U_3, \\ \dot{e}_{44} &= -10e_{22} + 0.15y_1y_3 - 0.15x_1x_3 - 0.3y_3y_5 + 0.3x_3x_5 + U_4, \\ \dot{e}_{55} &= -y_1 + x_1 + U_5. \end{aligned} \quad (23)$$

Theorem 2. *The control laws of (21) in switch-1 are chosen as follows*

$$
\begin{aligned}
U_1 &= -\hat{a}(y_2 - y_1) - 4y_2y_3 + ky_1\left(0.1 + 0.03{y_5}^2\right) - \hat{b}x_3 + x_1x_2 \\
&\quad - x_1x_5 - x_2x_4 - k_1e_{13} - h_1\mathrm{sgn}(e_{13})|e_{13}|^{\mu}, \\
U_2 &= y_1 - x_1 - 16e_{22} - e_{24} + y_1y_3 - x_1x_3 - k_2e_{22} - h_2\mathrm{sgn}(e_{22})|e_{22}|^{\mu}, \\
U_3 &= \hat{b}y_3 - y_1y_2 + y_1y_5 + y_2y_4 + \hat{a}(x_2 - x_1) + 4x_2x_3 \\
&\quad + kx_1\left(0.1 + 0.03{x_5}^2\right) - k_3e_{31} - h_3\mathrm{sgn}(e_{31})|e_{31}|^{\mu}, \\
U_4 &= 10e_{22} - 0.15y_1y_3 + 0.15x_1x_3 + 0.3y_3y_5 - 0.3x_3x_5 \\
&\quad - k_4e_{44} - h_4\mathrm{sgn}(e_{44})|e_{44}|^{\mu}, \\
U_5 &= y_1 - x_1 - k_5e_{25} - h_5\mathrm{sgn}(e_{55})|e_{55}|^{\mu}.
\end{aligned} \tag{24}
$$

where $k_i (i = 1 \cdots 5)$ and $h_i (i = 1 \cdots 5)$ are the positive constants, $0 < \mu < 1$, $\hat{a}(t)$ and $\hat{b}(t)$ are the estimated values of the unknown parameters a and b, respectively.

The parameters update laws are designed as

$$
\begin{aligned}
\dot{\hat{a}}(t) &= e_{13}(y_2 - y_1) - e_{31}(x_2 - x_1), \\
\dot{\hat{b}}(t) &= e_{13}x_3 - e_{31}y_3.
\end{aligned} \tag{25}
$$

Proof. Substituting (23) into (22) yields

$$
\begin{aligned}
\dot{e}_{13} &= \tilde{a}(t)(y_2 - y_1) + \tilde{b}(t)x_3 - k_1e_{13} - h_1\mathrm{sgn}(e_{13})|e_{13}|^{\mu}, \\
\dot{e}_{22} &= -k_{22}e_{22} - h_2\mathrm{sgn}(e_{22})|e_{22}|^{\mu}, \\
\dot{e}_{31} &= -\tilde{b}(t)y_3 - \tilde{a}(t)(x_2 - x_1) - k_2e_{31} - h_3\mathrm{sgn}(e_{31})|e_{31}|^{\mu}, \\
\dot{e}_{44} &= -k_4e_{44} - h_4\mathrm{sgn}(e_{44})|e_{44}|^{\mu}, \\
\dot{e}_{55} &= -k_5e_{55} - h_5\mathrm{sgn}(e_{55})|e_{55}|^{\mu},
\end{aligned} \tag{26}
$$

where $\tilde{b}(t) = b - \hat{b}(t)$ and $\tilde{a}(t) = a - \hat{a}(t)$ are parameter errors, correspondingly, $\dot{\tilde{b}}(t) = -\dot{\hat{b}}(t)$ and $\dot{\tilde{a}}(t) = -\dot{\hat{a}}(t)$.

A candidate Lyapunov function is considered as follows,

$$
V = \frac{1}{2}\left({e_{13}}^2 + {e_{22}}^2 + {e_{31}}^2 + {e_{44}}^2 + {e_{55}}^2 + \tilde{a}^2 + \tilde{b}^2\right). \tag{27}
$$

Then

$$
\begin{aligned}
\dot{V} &= e_{13}\dot{e}_{13} + e_{22}\dot{e}_{22} + e_{31}\dot{e}_{31} + e_{44}\dot{e}_{44} + e_{55}\dot{e}_{55} + \tilde{a}\dot{\tilde{a}} + \tilde{b}\dot{\tilde{b}}, \\
&= e_{13}\left(\tilde{a}(y_2 - y_1) + \tilde{b}x_3 - k_1e_{13} - h_1\mathrm{sgn}(e_{13})|e_{13}|^{\mu}\right) - k_2{e_{22}}^2 - h_2|e_{22}|^{\mu+1} \\
&\quad + e_{31}\left(-\tilde{b}y_3 - \tilde{a}(x_2 - x_1) - k_2e_{31} - h_3\mathrm{sgn}(e_{31})|e_{31}|^{\mu}\right) \\
&\quad - k_4{e_{44}}^2 - h_4|e_{44}|^{\mu+1} - k_5{e_{55}}^2 - h_5|e_{55}|^{\mu+1} + \tilde{a}\dot{\tilde{a}} + \tilde{b}\dot{\tilde{b}}, \\
&= -k_1{e_{13}}^2 - k_2{e_{22}}^2 - k_3{e_{31}}^2 - k_4{e_{44}}^2 - k_5{e_{55}}^2 \\
&\quad + \tilde{a}(e_{13}(y_2 - y_1) - e_{31}(x_2 - x_1)) \\
&\quad - \tilde{b}(e_{13}x_3 - e_{31}y_3) + \tilde{a}\dot{\tilde{a}} + \tilde{b}\dot{\tilde{b}} - h_1|e_{13}|^{\mu+1} \\
&\quad - h_2|e_{22}|^{\mu+1} - h_3|e_{31}|^{\mu+1} - h_4|e_{44}|^{\mu+1} - h_5|e_{55}|^{\mu+1}, \\
&= -k_1{e_{13}}^2 - k_2{e_{22}}^2 - k_3{e_{31}}^2 - k_4{e_{44}}^2 - k_5{e_{55}}^2 \\
&\quad + \tilde{a}\left(e_{13}(y_2 - y_1) - e_{31}(x_2 - x_1) - \dot{\hat{a}}\right) - \tilde{b}\left(e_{13}x_3 - e_{31}y_3 - \dot{\hat{b}}\right) \\
&\quad - h_1|e_{13}|^{\mu+1} - h_2|e_{22}|^{\mu+1} - h_3|e_{31}|^{\mu+1} - h_4|e_{44}|^{\mu+1} - h_5|e_{55}|^{\mu+1}.
\end{aligned} \tag{28}
$$

Substituting (23) into (26) gains

$$
\begin{aligned}
\dot{V} &= e_{13}\dot{e}_{13} + e_{22}\dot{e}_{22} + e_{31}\dot{e}_{31} + e_{44}\dot{e}_{44} + e_{55}\dot{e}_{55} + \tilde{a}\dot{\tilde{a}} + \tilde{b}\dot{\tilde{b}}, \\
&= -k_1{e_{13}}^2 - k_2{e_{22}}^2 - k_3{e_{31}}^2 - k_4{e_{44}}^2 - k_5{e_{55}}^2 - h_1|e_{13}|^{\mu+1} \\
&\quad - h_2|e_{22}|^{\mu+1} - h_3|e_{31}|^{\mu+1} - h_4|e_{44}|^{\mu+1} - h_5|e_{55}|^{\mu+1} \le -K\|e\|^2 \le 0,
\end{aligned} \tag{29}
$$

where $K = \min\{k_1, k_2, k_3, k_4, k_5 | k_i \in R^+, i = 1, 2, \cdots, 5\}$. Thus, it is obvious that $\dot{V}$ is negative definite. According to the Lyapunov stability theory, $\lim_{t\to\infty} \|e(t)\| = 0$ which means that the adaptive multi-switching synchronization of the master-slave hyperchaotic system is implemented. The analysis of the linear dependence condition for the parameter identification is follows as

$$
\begin{aligned}
&e_{13} = 0|_{t\to\infty}, e_{22} = 0|_{t\to\infty}, e_{31} = 0|_{t\to\infty}, e_{44} = 0|_{t\to\infty}, \\
&e_{55} = 0|_{t\to\infty},
\end{aligned} \tag{30}
$$

$$
\begin{aligned}
\dot{e}_{13} &= \tilde{a}(t)(y_2 - y_1) + \tilde{b}(t)x_3 - k_1e_{13} - h_1\mathrm{sgn}(e_{13})|e_{13}|^{\mu} = 0, \\
\dot{e}_{22} &= -k_{22}e_{22} - h_2\mathrm{sgn}(e_{22})|e_{22}|^{\mu} = 0, \\
\dot{e}_{31} &= -\tilde{b}(t)y_3 - \tilde{a}(t)(x_2 - x_1) - k_2e_{31} - h_3\mathrm{sgn}(e_{31})|e_{31}|^{\mu} = 0, \\
\dot{e}_{44} &= -k_4e_{44} - h_4\mathrm{sgn}(e_{44})|e_{44}|^{\mu} = 0, \\
\dot{e}_{55} &= -k_5e_{55} - h_5\mathrm{sgn}(e_{55})|e_{55}|^{\mu} = 0.
\end{aligned} \tag{31}
$$

For $y_2 \neq y_1, x_3 \neq 0, y_3 \neq 0, x_2 \neq x_1$, according to the linear independence conditions, $\tilde{a}(t) = 0$, $\tilde{b}(t) = 0$, hence $\hat{b}(t) = b$ and $\hat{a}(t) = a$, the parameters can be identified to the true values.

Remark 5. Since (24) contains a discontinuous sign function that causes an unwanted chattering. To avoid thrashing, replace sign functions with continuous *tanh* function to eliminate discontinuities. Therefore, the control law (24) is amended as follows:

$$
\begin{aligned}
U_1 &= -\hat{a}(y_2 - y_1) - 4y_2y_3 + ky_1\left(0.1 + 0.03{y_5}^2\right) - \hat{b}x_3 \\
&\quad + x_1x_2 - x_1x_5 - x_2x_4 - k_1e_{13} - h_1\tanh(e_{13})|e_{13}|^{\mu}, \\
U_2 &= y_1 - x_1 - 16e_{22} - e_{24} + y_1y_3 - x_1x_3 - k_2e_{22} - h_2\tanh(e_{22})|e_{22}|^{\mu}, \\
U_3 &= \hat{b}y_3 - y_1y_2 + y_1y_5 + y_2y_4 + \hat{a}(x_2 - x_1) + 4x_2x_3 \\
&\quad + kx_1\left(0.1 + 0.03{x_5}^2\right) - k_3e_{31} - h_3\tanh(e_{31})|e_{31}|^{\mu}, \\
U_4 &= 10e_{22} - 0.15y_1y_3 + 0.15x_1x_3 + 0.3y_3y_5 - 0.3x_3x_5 \\
&\quad - k_4e_{44} - h_4\tanh(e_{44})|e_{44}|^{\mu}, \\
U_5 &= y_1 - x_1 - k_5e_{25} - h_5\tanh(e_{55})|e_{55}|^{\mu}.
\end{aligned} \tag{32}
$$

Corollary 2. *For switch-2, the dynamic equation error is represented as*

$$
\begin{aligned}
\dot{e}_{12} &= a(y_2 - y_1) + 4y_2y_3 - ky_1\left(0.1 + 0.03{y_5}^2\right) + x_1 \\
&\quad - 16x_2 + x_1x_3 - x_4 + U_1, \\
\dot{e}_{23} &= -y_1 + 16y_2 - y_1y_3 + y_4 + bx_3 - x_1x_2 + x_1x_5 + x_2x_4 + U_2, \\
\dot{e}_{34} &= -by_3 + y_1y_2 - y_1y_5 - y_2y_4 + 10x_2 - 0.15x_1x_3 + gx_3x_5 + U_3, \\
\dot{e}_{45} &= -10y_2 + 0.15y_1y_3 - gy_3y_5 + x_1 + U_4, \\
\dot{e}_{51} &= -y_1 - a(x_2 - x_1) - 4x_2x_3 + kx_1\left(0.1 + 0.03{x_5}^2\right) + U_5.
\end{aligned} \tag{33}
$$

Theorem 3. *The control laws of (32) are chosen as follows:*

$$
\begin{aligned}
U_1 &= -\hat{a}(y_2 - y_1) - 4y_2y_3 + ky_1\left(0.1 + 0.03{y_5}^2\right) - x_1 + 16x_2 \\
&\quad - x_1x_3 + x_4 - k_1e_{12} - h_1\tanh(e_{12})|e_{12}|^{\mu}, \\
U_2 &= y_1 - 16y_2 + y_1y_3 - y_4 + \hat{b}x_3 + x_1x_2 - x_1x_5 - x_2x_4 - k_2e_{23} \\
&\quad - h_2\tanh(e_{23})|e_{23}|^{\mu}, \\
U_3 &= \hat{b}y_3 - y_1y_2 + y_1y_5 + y_2y_4 - 10x_2 + 0.15x_1x_3 - gx_3x_5 \\
&\quad - k_3e_{34} - h_3\tanh(e_{34})|e_{34}|^{\mu}, \\
U_4 &= 10y_2 - 0.15y_1y_3 + gy_3y_5 - x_1 - k_4e_{45} - h_4\tanh(e_{45})|e_{45}|^{\mu}, \\
U_5 &= y_1 + \hat{a}(x_2 - x_1) + 4x_2x_3 - kx_1\left(0.1 + 0.03{x_5}^2\right) \\
&\quad - k_5e_{51} - h_5\tanh(e_{51})|e_{51}|^{\mu},
\end{aligned} \tag{34}
$$

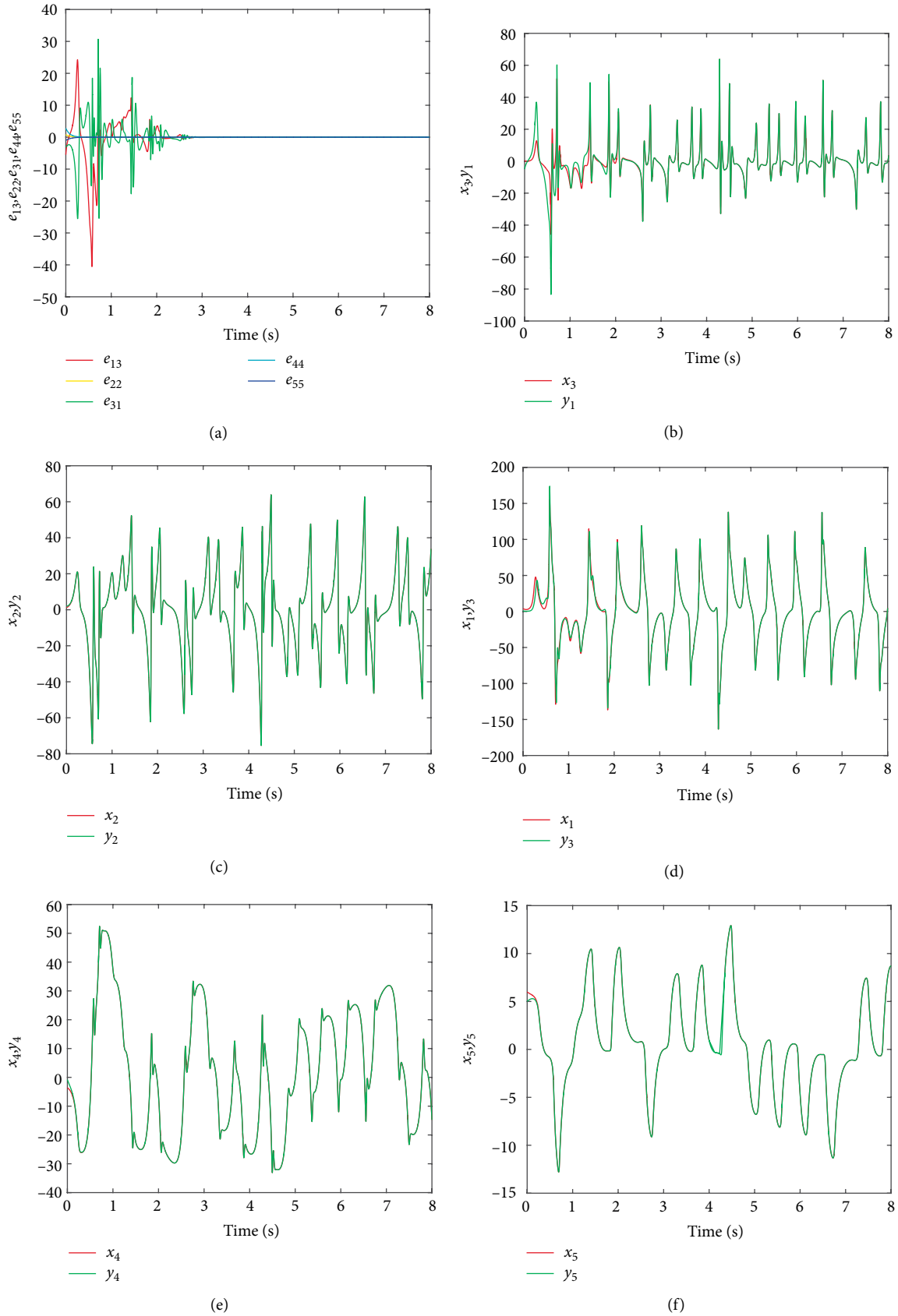

FIGURE 5: Switch-1: (a) the synchronization error, (b) the error of $x_3 - y_1$, (c) the error of $x_2 - y_2$, (d) the error of $x_1 - y_3$, (e) the error of $x_4 - y_4$, (f) the error of $x_5 - y_5$.

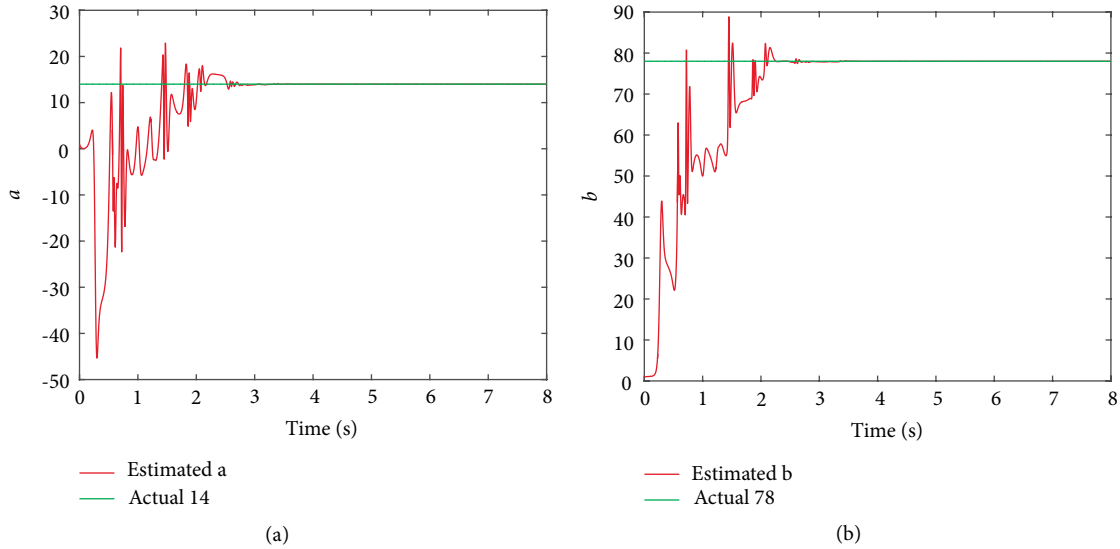

(a) (b)

Figure 6: Switch-1: (a) unknown term a, (b) unknown term b.

where $k_i (i = 1 \cdots 5)$ and $h_i (i = 1 \cdots 5)$ are the positive constant, $0 < \mu < 1$, $\hat{a}(t)$, and $\hat{b}(t)$ are the estimated value of the unknown parameters a and b respectively.

Meanwhile, parameters update laws of the unknown parameters are selected as

$$\begin{aligned} \dot{\hat{a}}(t) &= e_{12}(y_2 - y_1) - e_{51}(x_2 - x_1), \\ \dot{\hat{b}}(t) &= e_{23}x_3 - e_{34}y_3. \end{aligned} \tag{35}$$

Remark 6. The proof of switch-2 is the same as that of switch-1, and finally $e(t) \to 0$, the adaptive multi-switching synchronization for the master-slave system is implemented.

3.3. Simulation Results. The initial values of (19) and (20) are taken as $x(0) = [4, 1.2, 0.5, -3.6, 6]^T$ and $y(0) = [-5, 2, 1, -0.8, 5]^T$ respectively. The parmeters $K = k_i = 10\ (i = 1 \cdots 5), h_i = 2\ (i = 1 \cdots 5), \mu = 0.5$ are selected simultaneously.

Case 1. For switch-1, the synchronization of two 5D memristor hyperchaotic systems is implemented at 2.8 s in Figure 5. The unknown parameters a and b of the master-slave synchronization system are identified to their given values 14 and 78 respectively in Figure 6.

Case 2. For switch-2, Figure 7 demonstrates the synchronization of two 5D memristor hyperchaotic systems, the dynamic error of the system can reach to zero at 1.4 s. Figure 8 indicates that the uncertain parameters a, b can arrive at 14, 78 respectively when $a = 14$ and $b = 78$.

Remark 7. The above description illustrates that the synchronization of two 5D memristor hyperchaotic systems with unknown parameters is achieved by the adaptive control in each switching form, the uncertain parameters can converge to their given values simultaneously. For multi-switching synchronization can offer various combinations of the dynamics errors, which is very difficult to get or modify useful information for intruders, the adaptive multi-switching synchronization strategy is suitable for applying in secure communication.

4. Applications in Secure Communication

Due to the importance of information, information confidentiality is particularly important in secure communication. The essence of secure communication is to encrypt the transmitted information in some way. The concealment, unpredictability, high complexity, and easy implementation of hyperchaotic signals are especially suitable for secure communication. Hyperchaotic encryption is a dynamic encryption method, the encrypted information is difficult to decipher and has a high density in this way. In order to recover the original information, the decryption process is very important and can be realized by hyperchaotic synchronization scheme [36].

In the following sections, masking encryption and image encryption are discussed based on adaptive multi-switching synchronization of hyperchaotic systems with memristors.

4.1. Chaotic Masking Encryption and Decryption. The schematic diagram of hyperchaotic masking secure communication [37] is shown in Figure 9. The communication system is consisted by a transmitter which is a master system and a receiver which is a slave system, an output signal of the master system is acted as a masking signal to mask a message signal, the transmitted signal is a mixed output of a useful signal, and a hyperchaotic signal. In the receiver, the corresponding chaotic synchronization signal is employed to decrypt the mixed signals, ultimately, the original message signal is recovered.

In this work, the message signal is selected as a sinusoidal function which can be recovered in the receiver. The chaotic signal x is taken as the masking signal, then the encrypted signal $s_m(t) = s_i(t) + x$. In the receiver, the chaotic signal y is taken as the decrypt signal, the final output signal of the

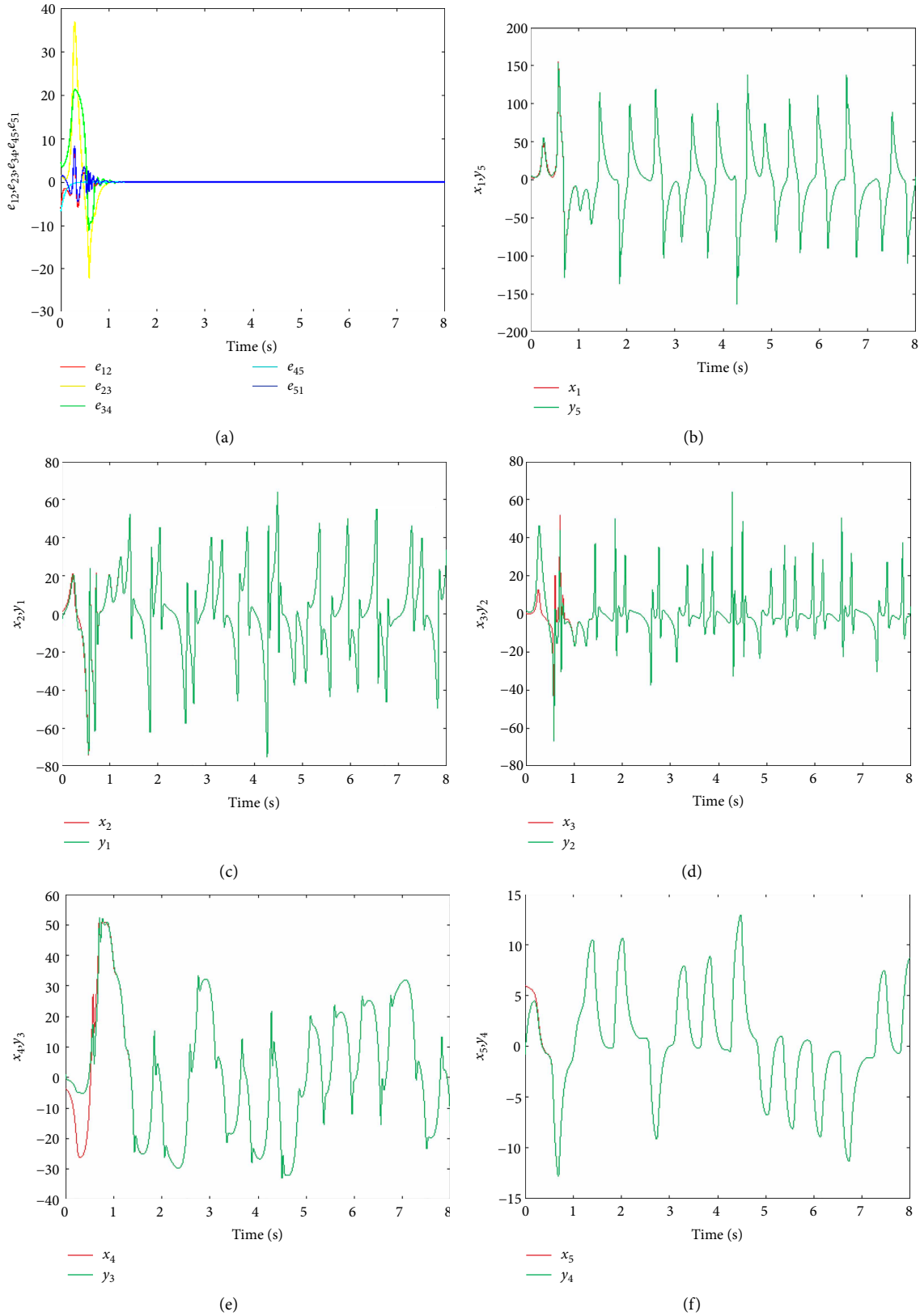

FIGURE 7: Switch-2: (a) the synchronization error, (b) the error of $x_1 - y_5$, (c) the error of $x_2 - y_1$, (d) the error of $x_3 - y_2$, (e) the error of $x_4 - y_3$, (f) the error of $x_5 - y_4$.

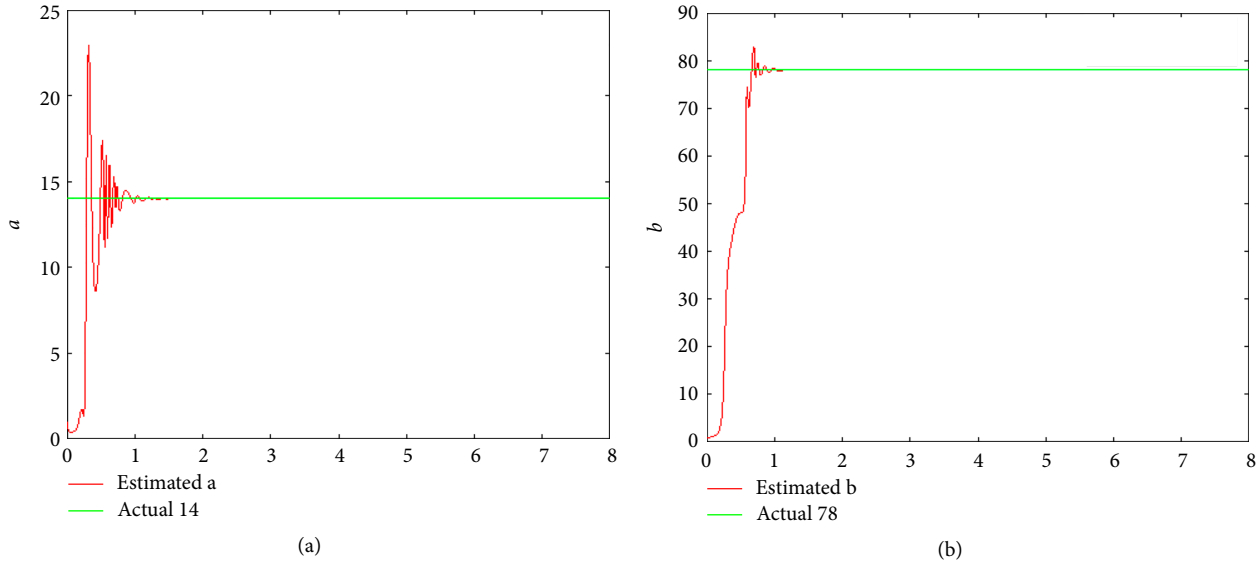

Figure 8: Switch-2: (a) unknown term a, (b) unknown term b.

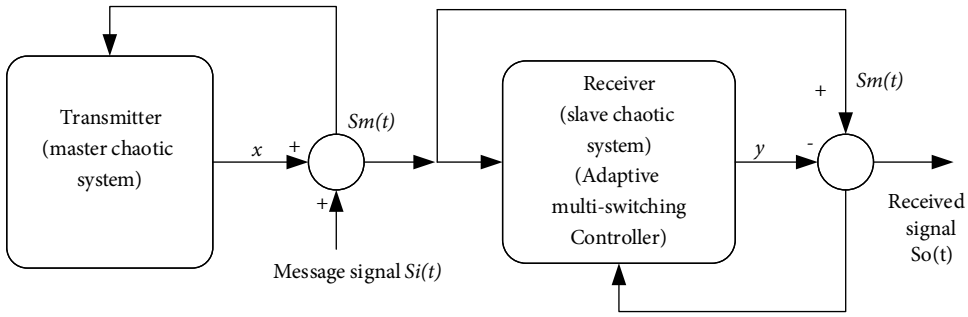

Figure 9: The schematic diagram of hyperchaotic masking secure communication.

receiver $s_o(t)$ can be calculated by $s_0(t) = s_m(t) - y$. When system (19) and (20) reach the adaptive synchronization, then $y - x \to 0$ and $s_0 = s_i$, the numerical simulation results are demonstrated in Figures 10 and 11.

4.2. Image Encryption and Decryption. In 1997, Fridrich composited chaos theory and image encryption to propose a chaotic image encryption method for the first time [38]. The potential application value of high order hyperchaotic system in image processing has been deeply studied, because it has more complex dynamics, more positive Lyapunov exponents, larger Kolmogorov entropy, and more sensitive to initial values. This subsection verifies the effectiveness of image encryption algorithm about the adaptive multi-switching hyperchaotic synchronization with memristors. The overall structure of image encryption and decryption process is shown in Figure 12.

4.2.1. The Process of Image Encryption. The detailed steps of the image encryption are as follows:

(a) Read the 3-color data matrices R, G, B of the original image with $256 \times 256 \times 3$ pixels.

(b) Gain the 5-dimmensional different chaotic sequences from $x = [x_1, x_2, x_3, x_4, x_5]^T$, then convert each chaotic sequence of x_1, x_2, x_3 into a two-dimensional sequence of rows and columns, and confuse them by ascending order or descending order, finally get the cipher text matrices R', G', B' of the original image.

(c) Replace the pixel values by chaotic sequence x_4. First take two parameters c and d as follows

$$\begin{cases} c_{ij} = abs(x_4(i,j) - round(x_4(i,j))) \times 10^2, \\ d_{ij} = abs(x_4(i,j) - round(x_4(i,j))) \times 10^3, \end{cases} \quad (36)$$

(d) The matrix of intermediate variables A is assumed as follows

$$A = \left(c_{ij} \times i + d_{ij} \times j\right) \bmod L, \quad (37)$$

where i and j are row and column position of the pixel respectively, L Gray level of the pixel.
Complete the XOR operation between R', G', B', and A.

$$\begin{cases} R'' = R' \oplus A, \\ G'' = G' \oplus A, \\ B'' = B' \oplus A, \end{cases} \quad (38)$$

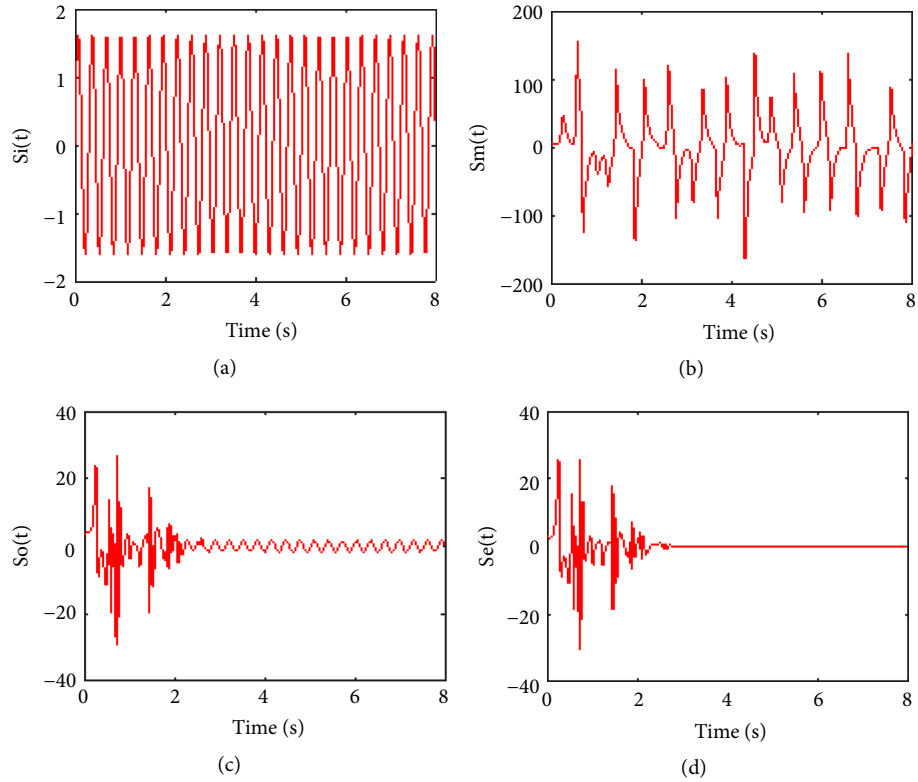

FIGURE 10: Switch-1 (a) the message signal $s_i(t) = 1.6\sin(20t)$, (b) the encrypted signal $s_m(t)$, (c) the recovered signal $s_0(t)$, and (d) the error signal $s_e(t)$.

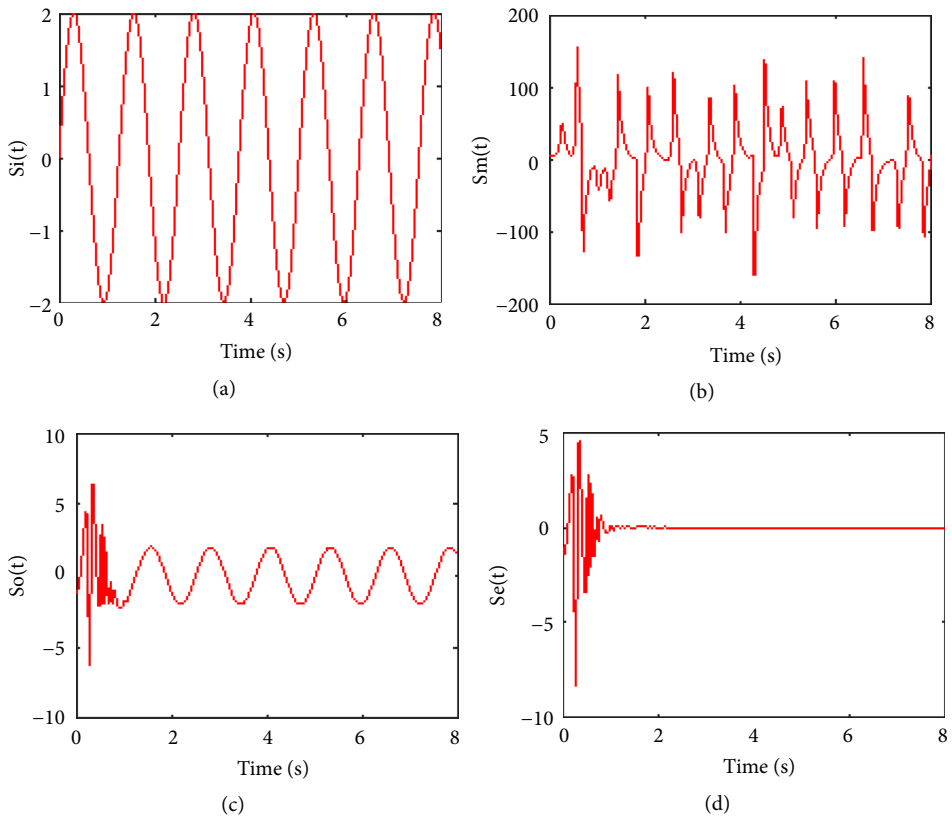

FIGURE 11: For switch-2 (a) The message signal $s_i(t) = 2\sin(5t)$, (b) the encrypted signal $s_m(t)$, (c) the recovered signal $s_0(t)$, and (d) the error signal $s_e(t)$.

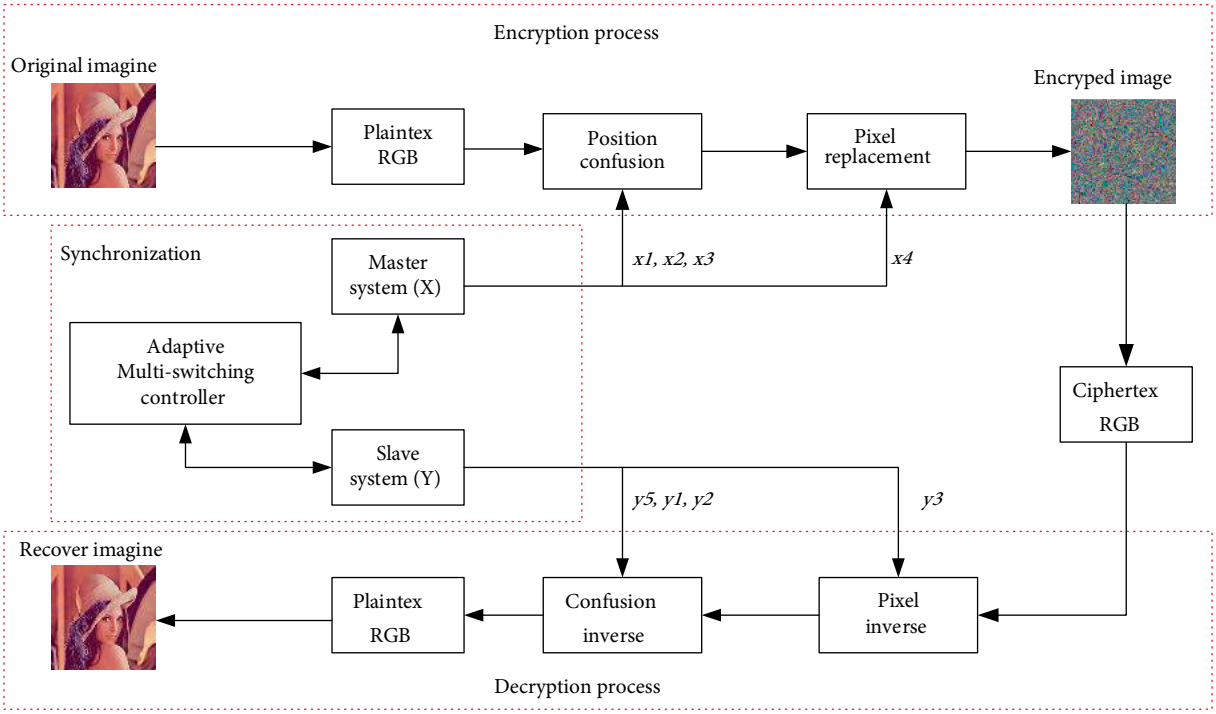

Figure 12: The overall structure of image encryption and decryption.

Table 1: XOR operation.

R'	G'	B'	A	$R'' = R' \oplus A$	$G'' = G' \oplus A$	$B'' = B' \oplus A$
0	0	0	0	1	1	1
0	0	0	1	0	0	0
1	1	1	0	0	0	0
1	1	1	1	1	1	1

Table 2: XOR operation.

R'''	G'''	B'''	A'	$R'' = R''' \oplus A'$	$G'' = G''' \oplus A'$	$B'' = B''' \oplus A'$
0	0	0	0	1	1	1
0	0	0	1	0	0	0
1	1	1	0	0	0	0
1	1	1	1	1	1	1

where R'', G'' and B'' are 3-color matrices of the encrypted image.
XOR operation results are shown in Table 1.

(e) Convert the binary sequences into the 2-dimension matrices R''', G''', and B'''.

(f) Finally restructure the 2-dimension matrices R''', G''', and B''', then obtain an encrypted image.

4.2.2. The Process of Image Decryption. Image encryption specific steps are as follows:

(a) Read the 3-color cipher text matrices R''', G''', and B''' of the encrypted image with $256 \times 256 \times 3$ pixels.

(b) Gain the 5-dimmensional different chaotic sequences from $y = [y_1, y_2, y_3, y_4, y_5]^T$, then convert each chaotic sequence of y_3 into a two-dimensional sequence of rows and columns.

(c) Recover the pixel values by chaotic sequence y_3. First take two parameters c'_{ij} and d'_{ij} as follows

$$\begin{cases} c'_{ij} = abs(y_3(i,j) - round(y_3(i,j))) \times 10^2, \\ d'_{ij} = abs(y_3(i,j) - round(y_3(i,j))) \times 10^3, \end{cases} \quad (39)$$

(d) The matrix of intermediate variables A' is assumed as follows

$$A' = \left(c'_{ij} \times i + d'_{ij} \times j\right) \bmod L, \quad (40)$$

where i and j are row and column position of the pixel respectively, L Gray level of the pixel.

Accomplish the XOR operation between R'', G'', and B'' and A'.

$$\begin{cases} R'' = R''' \oplus A', \\ G'' = G''' \oplus A', \\ B'' = B''' \oplus A', \end{cases} \quad (41)$$

where R'', G'', and B'' are 3-color matrices of the decrypted image.
XOR operation results are shown in Table 2.

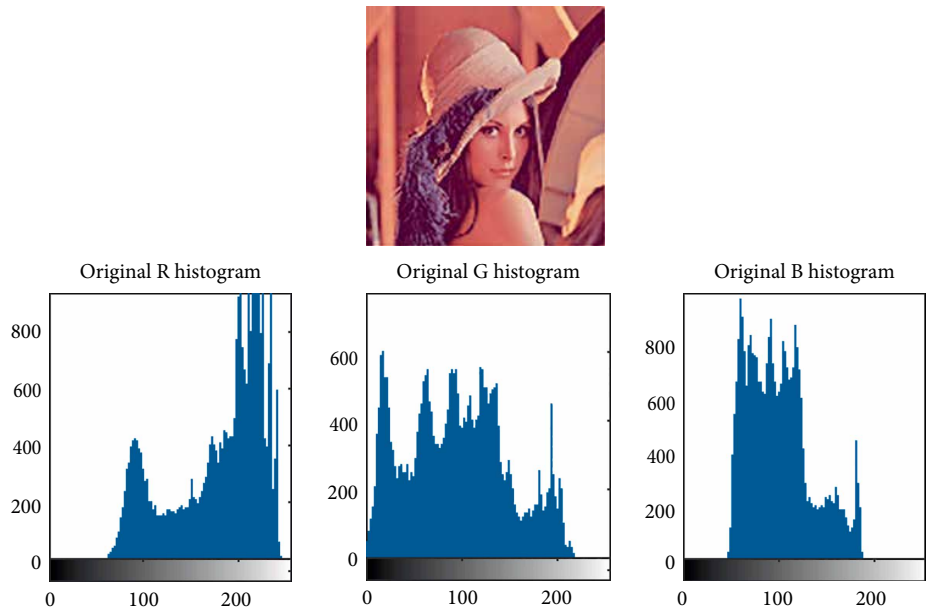

Figure 13: The original image with its histograms of color image (reproduced from Jing Luo et al. (2019), (under the Creative Commons Attribution License/public domain)).

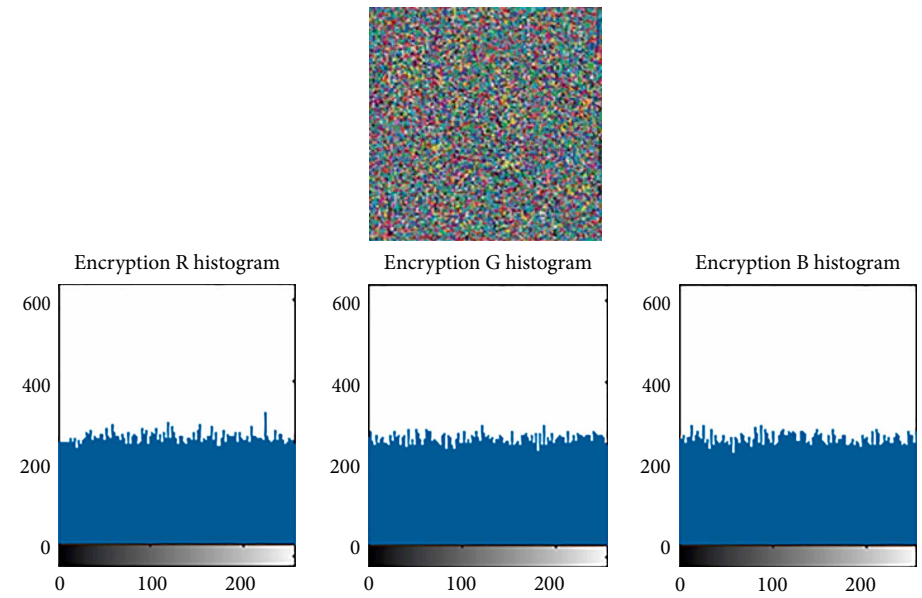

Figure 14: The encrypted image with its histograms (reproduced from Jing Luo et al. (2019), (under the Creative Commons Attribution License/public domain)).

(e) Convert the binary sequences into the 2-dimension matrices R', G', and B'.

(f) Sort the matrices of y_5, y_1, y_2, in descending order and ascending order as column confusion indexes to recover the cipher text image from R', G', and B', then gain R, G, B plaintext matrix.

(g) Finally restructure the 2-dimension matrices R, G, B, then obtain an decrypted image.

4.3. Analysis of the Image. Image histogram analysis and correlation coefficient analysis are two important statistical methods during the process of image encryption and decryption. By image histogram analysis, Figures 13–15 indicated the effects and performance of image encryption and decryption. Among them, Figure 13 demonstrates the histograms of the original image with uneven distribution, but Figure 14 shows uniform distribution of the encrypted image. After recovering the encrypted image, Figure 15 indicates that the decrypted image and its histograms is the same with Figure 13.

For the pixels are concentrated in original image with higher correlation distribution between adjacent pixels, in order to resist external attack, the correlation of adjacent pixels are reduced by image encryption strategy. 2000 pairs of

Figure 15: The decrypted image with its histograms (reproduced from Jing Luo et al. (2019), (under the Creative Commons Attribution License/public domain)).

Table 3: Correlation coefficient results.

Correlation	Original image	Encryption image	Original image [39]	Encryption image [39]
Horizontal	0.9748	0.0230	0.9856	−0.0 318
Vertical	0.9511	0.0226	0.9682	0.0965
Diagonal	0.9105	0.0105	0.9669	0.0362

adjacent pixels are chosen from the original image and encrypted image respcetively [36], the correlation coefficient can be calculated by (42). An interesting phenomenon is that the correlation coefficient of the original image in Table 3 is approximate to one. However, that of encrypted image is nearly equal to zero. Figures 16(b), 16(d), and 16(f) indicate that adjacent pixels of encrypted image are evenly distributed, Figures 16(a), 16(c), and 16(e) show that those of orignal image are higher correlation distribution.

$$\begin{aligned} E(v) &= \frac{1}{M}\sum_{i=1}^{M} w_i, \\ D(v) &= \frac{1}{M}\sum_{i=1}^{M} \left(v_i - E(v)\right)^2, \\ \operatorname{cov}(v,v) &= \frac{1}{M}\sum_{i=1}^{M} \left(a_i - E(v)\right)\left(v_i - E(v)\right), \\ R_{vw} &= \frac{\operatorname{cov}(v,w)}{\sqrt{D(v)} \times \sqrt{D(w)}}, \end{aligned} \tag{42}$$

where v and w are grey values between adjacent pixels, $E(v)$ is mathematical expectation, $\operatorname{cov}(v,w)$ is covariance, $D(v)$ is variance.

Remark 8. Literature [31] only presented adaptive synchronization design and simulation without considering its application. Literature [21] realized signal masking encryption by multi-switching chaos synchronization, not premeditating image encryption scheme. Compare with literature [39], Table 1 indicates the correlation coefficient in this section is lower. In this section, the adaptive multi-switching memristor-based hyperchaotic system is not only applied to signal masking encryption but also image encryption, which improves the security in signal transmission and resists external attacks.

Remark 9. Image encryption and decryption process in other switches is the same to one in switch-1.

5. Conclusions

Researches of hyperchaotic synchronous with memristor have attracted great attentions in theory and engineering practice. According to the Lyapunov stability theory, this paper presents an adaptive multi-switching synchronization strategy for high-order hyperchaotic systems with uncertain parameters. The numerical simulation results illustrate that the dynamic errors of the systems can quickly converge to zero and the unknown parameters can also be identified to the true values, which validates the feasibility and effectiveness of the proposed method. At last, adaptive multi-switching synchronization for high-order hyperchaotic systems is applied to image encryption, which is more secure than conventional encryption methods.

Unknown parameters, external disturbances, and time-delay are unavoidable in engineering practice, finite-time robust multi-switching synchronization control for memristor hyperchaotic systems with unknown parameters, external disturbances, and time-delay is a challenging study. In the future, our research will focus on designing the complex circuit of hyperchaotic system with memristors to accomplish the multi-switching synchronization and its application in image encryption.

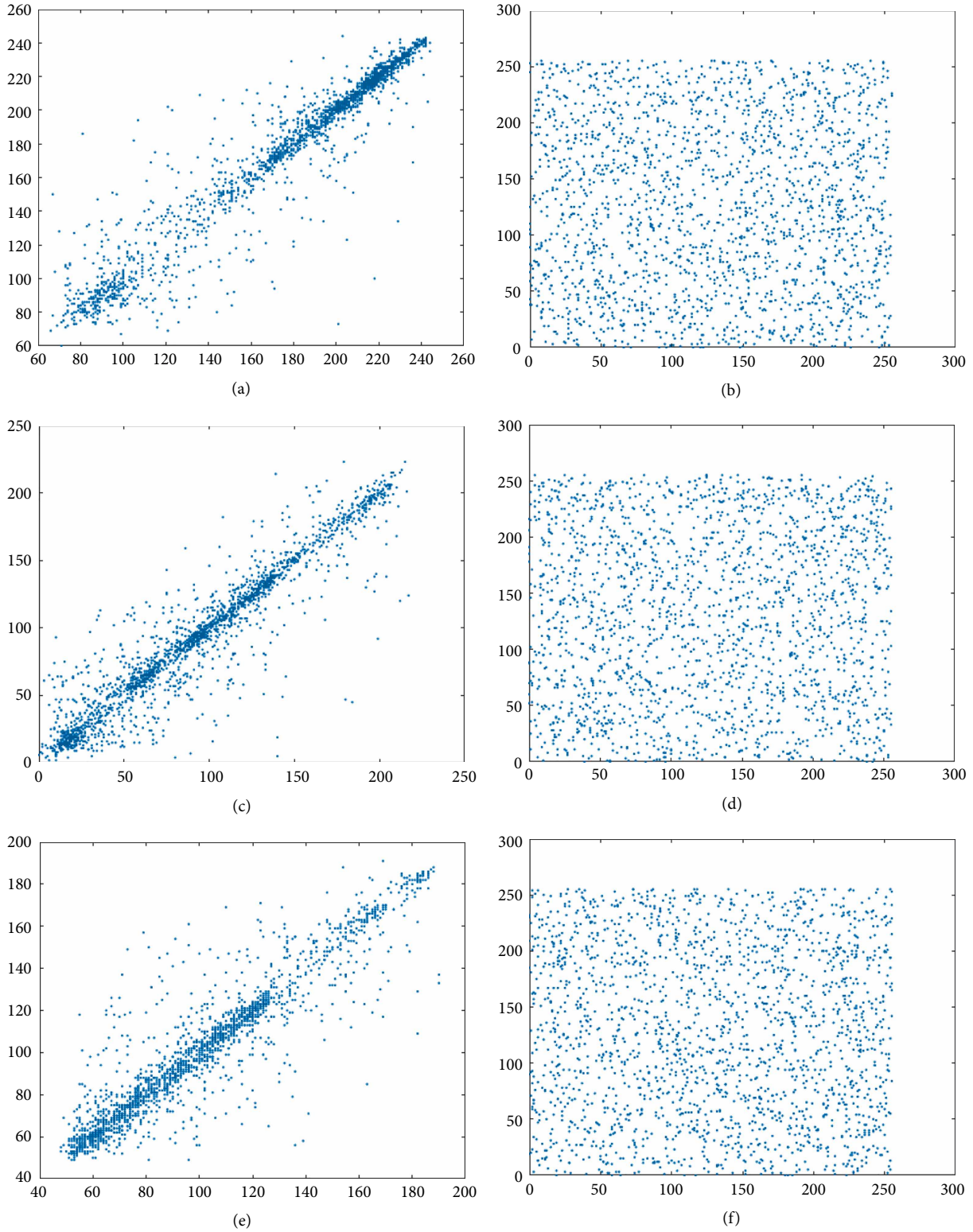

Figure 16: Horizontal correlation of original image. (a, c, e) are the correlation of original image in *RG*, and *B*, respectively; (b, d, f) are the correlation of encrypted image in *RG*, and *B*, respectively.

Data Availability

The data used to support the findings of this study are available from the corresponding author upon request.

Conflicts of Interest

The authors declare that there are no conflicts of interest regarding the publication of this paper.

Acknowledgments

This work was supported by National Natural Science Foundation of China under Grant Nos. 61673190/F03010, self-determined research funds of CCNU from the colleges' basic research and operation of MOE under Grant No. CCNU18TS042.

References

[1] L. M. Pecora and T. L. Carroll, "Synchronization in chaotic systems," *Controlling Chaos*, vol. 6, Elsevierpp. 142–145, 1996.

[2] J. Sun, Y. Shen, Q. Yin, and C. Xu, "Compound synchronization of four memristor chaotic oscillator systems and secure communication," *Chaos*, vol. 23, pp. 821–812, 2013.

[3] B. Lei and I. Y. Soon, "A multipurpose audio watermarking algorithm with synchronization and encryption," *Journal of Zhejiang University Science C Computers & Electronics*, vol. 13, no. 1, pp. 11–19, 2012.

[4] L. Wang, T. Dong, and M.-F. Ge, "Finite-time synchronization of memristor chaotic systems and its application in image encryption," *Applied Mathematics and Computation*, vol. 347, pp. 293–305, 2019.

[5] M. G. Rosenblum, A. S. Pikovsky, and J. Kurths, "Synchronization approach to analysis of biological systems," *Fluctuation & Noise Letters*, vol. 4, no. 1, pp. L53–L62, 2004.

[6] X. Xi, S. Mobayen, H. Ren, and S. Jafari, "Robust finite-time synchronization of a class of chaotic systems via adaptive global sliding mode control," *Journal of Vibration and Control*, vol. 24, pp. 3842–3854, 2017.

[7] J. Sun, W. Yan, Y. Wang, and S. Yi, "Finite-time synchronization between two complex-variable chaotic systems with unknown parameters via nonsingular terminal sliding mode control," *Nonlinear Dynamics*, vol. 85, no. 2, pp. 1105–1117, 2016.

[8] F. Min, C. Li, L. Zhang, and C. Li, "Initial value-related dynamical analysis of the memristor-based system with reduced dimensions and its chaotic synchronization via adaptive sliding mode control method," *Chinese Journal of Physics*, vol. 58, pp. 117–131, 2019.

[9] C. Li, X. Liao, and X. Zhang, "Impulsive synchronization of chaotic systems," *Chaos An Interdisciplinary Journal of Nonlinear Science*, vol. 15, no. 2, pp. 3031–382, 2006.

[10] S. Wen, Z. Zeng, T. Huang, and Y. Chen, "Fuzzy modeling and synchronization of different memristor-based chaotic circuits," *Physics Letters A*, vol. 377, no. 34-36, pp. 2016–2021, 2013.

[11] S. Wen, S. Xiao, Y. Yang, Z. Yan, Z. Zeng, and T. Huang, "Adjusting learning rate of memristor-based multilayer neural networks via fuzzy method," *IEEE Transactions on Computer-Aided Design of Integrated Circuits and Systems*, vol. 38, no. 6, pp. 1084–1094, 2019.

[12] A. Khan, D. Khattar, and N. Prajapati, "Adaptive multi switching combination synchronization of chaotic systems with unknown parameters," *International Journal of Dynamics and Control*, vol. 6, no. 2, pp. 621–629, 2018.

[13] S. Wen, Z. Zeng, and T. Huang, "Adaptive synchronization of memristor-based chua's circuits ," *Physics Letters A*, vol. 376, pp. 2775–2780, 2012.

[14] C. Li, F. Min, and C. Li, "Multiple coexisting attractors of the serial–parallel memristor-based chaotic system and its adaptive generalized synchronization," *Nonlinear Dynamics*, vol. 94, no. 4, pp. 2785–2806, 2018.

[15] U. Parlitz, "Estimating model parameters from time series by autosynchronization," *Physical Review Letters*, vol. 76, no. 8, pp. 1232–1235, 1996.

[16] H. Adloo and M. Roopaei, "Review article on adaptive synchronization of chaotic systems with unknown parameters," *Nonlinear Dynamics*, vol. 65, no. 1–2, pp. 141–159, 2011.

[17] W. Yu, G. Chen, J. Cao, J. Lu, and U. Parlitz, "Parameter identification of dynamical systems from time series," *Physical Review E Statistical, Nonlinear, biological, and Soft Matter Physics*, vol. 75, no. 6, p. 067201, 2007.

[18] Z. Sun, W. Zhu, G. Si, Y. Ge, and Y. Zhang, "Adaptive synchronization design for uncertain chaotic systems in the presence of unknown system parameters: a revisit," *Nonlinear Dynamics*, vol. 72, no. 4, pp. 729–749, 2013.

[19] A. Uçar, K. E. Lonngren, and E. W. Bai, "Multi-switching synchronization of chaotic systems with active controllers," *Chaos, Solitons & Fractals*, vol. 38, no. 1, pp. 254–262, 2008.

[20] X.-Y. Wang and P. Sun, "Multi-switching synchronization of chaotic system with adaptive controllers and unknown parameters," *Nonlinear Dynamics*, vol. 63, no. 4, pp. 599–609, 2011.

[21] I. Ahmad, M. Shafiq, and M. M. Al-Sawalha, "Globally exponential multi switching-combination synchronization control of chaotic systems for secure communications," *Chinese Journal of Physics*, vol. 56, no. 3, pp. 974–987, 2018.

[22] Y. Wen, X. Chen, J. Qiu, Z. Li, and C. Yang, "Multi-switching network transmission synchronization behavior for three uncertain chaotic systems with unknown parameters," in *Conference of the IEEE Industrial Electronics Society*, IEEEBeijing, China, 2017.

[23] A. Khan, M. Budhraja, and A. Ibraheem, "Multi-switching synchronization of four non-identical hyperchaotic systems," *International Journal of Applied & Computational Mathematics*, vol. 4, no. 2, p. 71, 2018.

[24] N. Prajapati, A. Khan, and D. Khattar, "On multi switching compound synchronization of non identical chaotic systems," *Chinese Journal of Physics*, vol. 56, no. 4, pp. 1656–1666, 2018.

[25] L. O. Chua, "Memristor-the missing circuit element," *IEEE Trans Circuit Theory*, vol. 18, no. 5, pp. 507–519, 1971.

[26] D. B. Strukov, G. S. Snider, D. R. Stewart, and R. S. Williams, "The missing memristor found," *Nature*, vol. 453, no. 7191, pp. 80–83, 2008.

[27] M. Itoh and L. O. Chua, "Memristor oscillators," *International Journal of Bifurcation & Chaos*, vol. 18, no. 11, pp. 3183–3206, 2008.

[28] S. Wen, R. Hu, Y. Yang, T. Huang, Z. Zeng, and Y.-D. Song, "Memristor-based echo state network with online least mean square," *IEEE Transactions on Systems, Man, and Cybernetics: Systems*, pp. 1–10, 2018.

[29] S. Wen, X. Xie, Z. Yan, T. Huang, and Z. Zeng, "General memristor with applications in multilayer neural networks," *Neural Networks*, vol. 103, pp. 142–149, 2018.

[30] J. Sun, X. Zhao, J. Fang, and Y. Wang, "Autonomous memristor chaotic systems of infinite chaotic attractors and circuitry realization," *Nonlinear Dynamics*, vol. 94, no. 4, pp. 2879–2887, 2018.

[31] R. Wang, M. Li, Z. Gao, and H. Sun, "A new memristor-based 5D chaotic system and circuit implementation," *Complexity*, vol. 2018, Article ID 6069401, 12 pages, 2018.

[32] S. Wen, S. Xiao, and Y. Yang, "Passivity and passification of memristive neural networks with leakage term and time-varying delays," *Applied Mathematics and Computation*, vol. 361, pp. 294–310, 2019, In press.

[33] J. Sun, S. Yi, Y. Quan, and C. Xu, "Compound synchronization of four memristor chaotic oscillator systems and secure communication," *Chaos: An Interdisciplinary Journal of Nonlinear Science*, vol. 23, no. 1, p. 013140, 2013.

[34] C. Li, F. Min, Q. Jin, and H. Ma, "Extreme multistability analysis of memristor-based chaotic system and its application in image decryption," *AIP Advances*, vol. 7, no. 12, p. 125204, 2017.

[35] J. Ma, Z. Chen, Z. Wang, and Q. Zhang, "A four-wing hyper-chaotic attractor generated from a 4-D memristive system with a line equilibrium," *Nonlinear Dynamics*, vol. 81, pp. 1275–1288, 2015.

[36] M. A. Murillo-Escobar, C. Cruz-Hernández, F. Abundiz-Pérez, R. M. López-Gutiérrez, and O. R. A. D. Campo, "A RGB image encryption algorithm based on total plain image characteristics and chaos," *Signal Processing*, vol. 109, pp. 119–131, 2015.

[37] Y. Fei and C. Wang, "Secure communication based on a four-wing chaotic system subject to disturbance inputs," *Optik-International Journal for Light and Electron Optics*, vol. 125, no. 20, pp. 5920–5925, 2014.

[38] J. Fridrich, "Symmetric ciphers based on two-dimensional chaotic maps," *International Journal of Bifurcation & Chaos*, vol. 8, no. 6, pp. 1259–1284, 1998.

[39] H. Liu and X. Wang, "Color image encryption based on one-time keys and robust chaotic maps," *Computers & Mathematics with Applications*, vol. 59, pp. 3320–3327, 2010.